Artificial Organs
••(••):••–••, Wiley Periodicals, Inc.

Pulsatile In Vitro Simulation of the Pediatric Univentricular Circulation for Evaluation of Cardiopulmonary Assist Scenarios

*Onur Dur, *Mikhail Lara, *Dorian Arnold, †Stijn Vandenberghe, *‡Bradley B. Keller, §Curt DeGroff, and *Kerem Pekkan

**Biomedical Engineering Department, Carnegie Mellon University, Pittsburgh, PA; †ARTORG Cardiovascular Engineering, University of Bern, Bern, Switzerland; ‡Cardiovascular Innovation Institute, University of Louisville, Louisville, KY; and §Congenital Heart Center, University of Florida, Gainesville, FL, USA*

Abstract: The characteristic depressed hemodynamic state and gradually declining circulatory function in Fontan patients necessitates alternative postoperative management strategies incorporating a system level approach. In this study, the single-ventricle Fontan circulation is modeled by constructing a practical in vitro bench-top pulsatile pediatric flow loop which demonstrates the ability to simulate a wide range of clinical scenarios. The aim of this study is to illustrate the utility of a novel single-ventricle flow loop to study mechanical cardiac assist to Fontan circulation to aid postoperative management and clinical decision-making of single ventricle patients. Two different pediatric ventricular assist devices, Medos and Pediaflow Gen-0, are anastomosed in two nontraditional configurations: systemic venous booster (SVB) and pulmonary arterial booster (PAB). Optimum ventricle assist device strategy is analyzed under normal and pathological (pulmonary hypertension) conditions. Our findings indicate that Medos ventricle assist device in SVB configuration provided the highest increase in pulmonary (46%) and systemic (90%) venous flow under normal conditions, whereas for the hypertensive condition, highest pulmonary (28%) and systemic (55%) venous flow augmentation were observed for the Pediaflow ventricle assist device inserted as a PAB. We conclude that mechanical cardiac assist in the Fontan circulation effectively results in flow augmentation and introduces various control modalities that can facilitate patient management. Assisted circulation therapies targeting single-ventricle circuits should consider disease state specific physiology and hemodynamics on the optimal configuration decisions. **Key Words:** Assisted circulation/methods—Fontan procedure/methods—Hemodynamics/physiology—Pulsatile flow—Ventricle-assist devices/utilization.

Single ventricle (SV) physiology introduces escalating energetic challenges in patients with congenital heart disease. The American Heart Association reports SV pathology as the leading cause of death from any birth defect less than 1 year of age (1) which requires the highest cost to treat any birth defect. Staged Fontan palliation has evolved based on the clinical experience and has become a routine approach for SV management. Despite progress in the last decades (2), outcomes remain suboptimal (3,4) due to inherently inefficient physiology. Often, patients in the immediate postoperative period suffer from acute heart failure as well as side effects as their cardiovascular system requires long periods for hemodynamic adjustment. Recently, increasing numbers of SV patients surviving into adulthood classified as "*failing* Fontans" pose severe deteriorating hemodynamic state, and require circulatory assist. Recent studies indicate that application of a pediatric ventricular assist device (PVAD) (5), propeller pump (6) or an intraaortic balloon pump (7) to the Fontan circuit may augment venous flow, improve

doi:10.1111/j.1525-1594.2009.00951.x

Received June 9; revised August 9.
Address correspondence and reprint requests to Assistant Professor Kerem Pekkan, Biomedical & Mechanical (courtesy) Engineering, School of Biomedical Engineering, Carnegie Mellon University, 2100 Doherty Hall, Pittsburgh, PA ••, USA. E-mail: kpekkan@andrew.cmu.edu

cavopulmonary connection with computational predictions. *Ann Biomed Eng* 2003;31:810–22.
32. Liu Y, Allaire P, Wood H, Olsen D. Design and initial testing of a mock human circulatory loop for left ventricular assist device performance testing. *Artif Organs* 2005;29:341–5.
33. Timms D, Hayne M, McNeil K, Galbraith A. A complete mock circulation loop for the evaluation of left, right, and biventricular assist devices. *Artif Organs* 2005;29:564–72.
34. du Plessis AJ, Chang AC, Wessel DL, et al. Cerebrovascular accidents following the Fontan operation. *Pediatr Neurol* 1995;12:230–6.
35. Hjortdal VE, Emmertsen K, Stenbog E, et al. Effects of exercise and respiration on blood flow in total cavopulmonary connection: a real-time magnetic resonance flow study. *Circulation* 2003;108:1227–31.
36. Hjortdal VE, Christensen TD, Larsen SH, Emmertsen K, Pedersen EM. Caval blood flow during supine exercise in normal and Fontan patients. *Ann Thorac Surg* 2008;85:599–603.
37. Hsia TY, Khambadkone S, Redington AN, Migliavacca F, Deanfield JE, de Leval MR. Effects of respiration and gravity on infradiaphragmatic venous flow in normal and Fontan patients. *Circulation* 2000;102:III148–53.
38. Penny DJ, Redington AN. Doppler echocardiographic evaluation of pulmonary blood flow after the Fontan operation: the role of the lungs. *Br Heart J* 1991;66:372–4.
39. Decramer M, De Troyer A, Kelly S, Zocchi L, Macklem PT. Regional differences in abdominal pressure swings in dogs. *J Appl Physiol* 1984;57:1682–7.

should quantify the acute volume shifts between each compartment to accurately evaluate hemodynamic adjustments and VAD performance. In addition, the indispensible effect of patient-specific anatomies (i.e., fabricating using rapid prototyping to match vascular impedance) (29) on Fontan hemodynamics which will critically influence the VAD selection should also be taken into account. Along this line, surgical templates of the intermediate high-risk stages (i.e., Norwood operation) can also be implemented in the current flow loop to explore the feasibility of PVAD implementation to support a single stage neonatal Fontan repair (9). As identified earlier, accurate description of the TCPC hemodynamics requires the simulation of respiration effects which remains as a challenging task to be implemented in future flow loop studies. Ongoing studies focus on performance of PVAD at novel deployment configurations such as the double inlet-double outlet configuration (which is an extension of the recent Optiflo conduit (30)) and the "ejector pump design" which uses the flow energy of one caval low to drive the other (Fig. 1).

Utility of distilled water in mock loops has been shown by several investigators (31–33). For the current study, the variation of viscosity affected only the pressure field as the bellows pump discharges constant flow rate regardless of the viscosity of the working fluid. Based on the comparative nature of this study, the variation in absolute pressure did not pose any limitation to the results presented. However, the effect of using lower viscosity fluid on the flow profile was negligible due to the typical high Womersley number (>10) in the large vessels. In addition, regardless of the relative increase in Reynolds number with the use of distilled water, turbulence phenomena have not been seen within any vessel segment. Also, the effects of polycythemia that is reported for some post-Fontan patients (34) were also not included. For a more precise study with exact patient specific parameters, a blood analog fluid and the changes in red blood cell rheology should be considered.

Although providing accurate local hemodynamic information along the entire SV circulation circuit, pulsatile venous flow waveforms clearly diverge from the actual in vivo waveforms acquired by Doppler Velocimetry (35). This is due to the neglecting of the high respiratory dependency (i.e., 30–100%) of the vena cavae flow in patients with TCPC (35–37) which stems from the variation of intrathoracic pressure (38) and abdominal pressure (39). Negative intrathoracic pressure during inspiration decreases the left atrial pressure and enhances both caval flows (18). Limited acute in vivo animal studies (unpublished data) have shown respiration to have a significant impact on the pulmonary impedance in the Fontan circulation. On the other hand, the increase in abdominal pressure produced by the descending diaphragm during inspiration enhances IVC flow substantially (37). Moreover, our recent numerical studies (22) revealed the indispensible effect of respiration and caval flow pulsatility on the internal energy dissipation inside the TCPC. Therefore, an accurate simulation of the TCPC hemodynamics requires inclusion of respiratory effects (35), a preload responsive cardiac simulator, and respiration dependant splanchnic venous return (37).

The current study has inherent limitations related to the selected devices and anastamotic configurations. The Pediaflow Gen-0 VAD provided a maximum output of 0.9 L/min at the highest settings and had high nonlinear pump resistance. Our study results indicate that in-line placement of the VAD in the venous conduit is sub-optimal and that alternative configurations where the VAD is placed in parallel with the existing flow conduit may be preferable. Future studies should consider the need to evaluate the change in loading conditions on the heart. In certain cases (such as dilated cardiomyopathy), increased loading of the ventricle may be quite detrimental in spite of any benefits derived from reduced pulmonary pressures or enhanced pulmonary perfusion. An elastance-based preload responsive ventricle should be coupled to our existing afterload model for this purpose. In spite of these limitations, this study demonstrates that mechanical support of Fontan patients is not a binary problem that can be addressed through LVAD support alone nor is it a matter of unloading the ventricle. VAD support in these patients should be based on balancing the perfusion needs of the patient and careful volume management of the major compartments of the circulatory system with the goal of unloading both the pulmonary circuit and heart.

CONCLUSION

For traditional adult VAD deployment, the location of anastomosis and pump selection in response to hemodynamics and physiology is a major current research interest and poses a very complex problem. Pediatric patients with congenital circulation malformations complicate the problem even further due to blood volume shifts, compliance remodeling during early post-op, control of venous collapse, unsteady venous flow dynamics and cardiopulmonary interactions. The proposed experimental setup provides a

deployment allowed slightly better pulmonary perfusion (4%). For hypertensive conditions, a similar conclusion, higher pulmonary flow increase with IVC deployment (15.5% vs. 12.4%) could be drawn. It is worth to note that average pulmonary pressure was 4 mm Hg higher in RPA configuration compared with the IVC deployment. For the Pediaflow VAD, PAB configuration allowed equally higher flow augmentation in caval veins (20–23%) and pulmonary arteries (30–48%) compared with SVB configuration under both normal and hypertensive conditions. Overall, these findings indicate that SVB configuration is more favorable for Medos VAD, whereas, PAB configuration should be preferred for Pediaflow VAD insertion as mechanical support.

VAD performance evaluation (Medos vs. Pediaflow)

In the SVB configuration, although the Pediaflow was capable of increasing the total CV flow (50% in normal and 29% in hypertensive condition), PA flow is not affected or even reduced in normal and hypertensive conditions, respectively. For RPA anastomosis, CV flow augmentation provided by the Pediaflow VAD is higher than Medos VAD: 91% versus 78% and 55% versus 51% with respect to normal and hypertensive conditions, respectively. In addition, Pediaflow VAD anastomosed at the RPA was notably more favorable in increasing PA flow under pulmonary hypertension (28% vs. 12%) and displayed the same performance as the Medos VAD in the normal conditions (both 46% PA flow increase). In summary, the Medos pump in IVC configuration provided the highest increase in PA (46%) and CV (90%) flow under normal conditions. Superiority of the Medos VAD in SVB configuration is primarily based on the active suction from the systemic circulation with this pulsatile VAD, and the increased adverse resistance introduced by continuous flow Pediaflow Gen-0. In contrast, for the hypertensive conditions, highest PA (28%) and CV (55%) flow augmentation is observed for the Pediaflow VAD inserted as a PAB. Hence, our study suggests that Pediaflow VAD in PAB configuration would be a better candidate for aiding hypertensive Failing Fontans, whereas, Medos VAD in SVB configuration should be considered for the immediate postoperative management of patients with functionally normal vascular conditions.

Pulsatility of Medos VAD over the steady PediaFlow discharge is another advantage that needs to be taken account in assisted support of the Fontan circuit. Along this line, insertion of PVADs to the Fontan circulation allowed modulation of flow waveforms along the TCPC pathway (i.e., IVC, SVC, RPA, and LPA). It is also found that the sinusoidal venous flow waveforms disappeared (i.e., steady flow) when the systemic venous compliance is increased. In contrast, pulsatile Medos VADs produced distinct flow waveforms and high pulsatility even in the high venous compliance condition (C >>10 mL/mm Hg) as shown in Fig. 6.

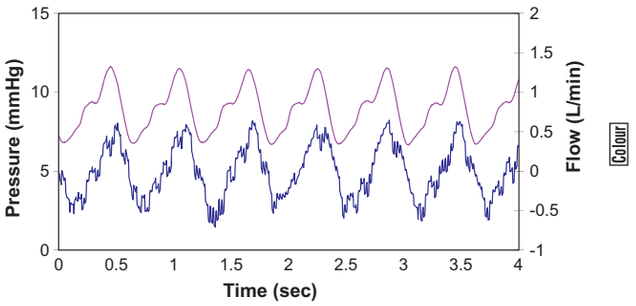

FIG. 6. Pressure (blue) and flow (red) waveforms measured at inferior vena cava (IVC) (top) and left pulmonary artery (LPA) (bottom) when Medos VAD inserted in systemic venous booster configuration.

Limitations and future directions

The present pulsatile in vitro Fontan flow loop demonstrated its utility to simulate the single-ventricle circulation and the hemodynamic effects of surgical interventions, including the PVAD assist to aid patients with degrading hemodynamics. However, at this stage, the main objective of this study was not to extract quantitative data on Fontan hemodynamics but to develop a versatile bench-top experimental setup with which we could compare alternative VAD performances and possible deployment configurations, thus to explore the feasibility of mechanical support in Fontan patients. There are several limitations in terms of the accuracy of the quantitative Fontan hemodynamics which need to be addressed in the future.

Although PVAD insertion confirmed increased pulmonary flow, cardiac output remained almost constant due to the lacking Frank-Starling mechanism under current settings of the flow loop. Minor increase in aortic flow (2.7%) after PVAD anastomosis is attributed to the active suction of fluid from the visceral circulation. More physiological ventricle function sensitive to afterload can be simulated by implementing a feedback-controlled positive-displacement pump (elastance-based control) as described by Baloa et al. (28). Albeit our qualitative observations confirmed the blood volume shift due venous congestion or VAD discharge, future studies

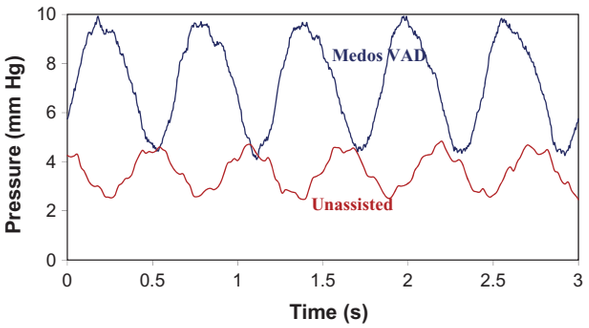

Colour

FIG. 5. LPA pressure for Medos VAD (blue) assisted circulation and unassisted circulation (red) under normal physiologic conditions.

pulmonary arteries was around 5 ± 3 mm Hg as shown in Fig. 5.

Pediaflow VAD anastomosis to the IVC segment caused adverse hemodynamics as the IVC flow decreased dramatically (–25%) causing venous stasis (i.e., volume shift) in the IVC compartment. In contrast, relatively larger cardiac output moved to visceral circulation, which increased the SVC flow substantially (106%). This allowed normal levels of pulmonary flow to be sustained in spite of the IVC flow reduction. However, Pediaflow insertion to RPA caused 49% reduction in RPA flow which is compensated by a dramatic increase in LPA flow (136%) based on the flow augmentation in both IVC (+54%) and SVC (+55%) segments. These nonintuitive results are primarily due to the increased (pulmonary) vascular resistance of the IVC (RPA) segments after VAD insertion due to the presence of the additional resistance of the pump itself. RPA deployment of Pediaflow VAD to aid pulmonary hypertension allowed 28% increase in overall pulmonary perfusion. In contrast, insertion through IVC caused further reduction in the pulmonary flow (–17%) due to the insufficient SVC flow augmentation (+71%) relative to the reduction in IVC flow (–25%). On average, pulmonary pressure was increased by 13 ± 7 mm Hg after Pediaflow VAD insertion.

DISCUSSION

Assisted cavopulmonary blood flow as a potential to serve as a bridge to neonatal SV Fontan repair (9,23–25) and long-term treatment option for failing Fontan physiology (26,27) has been demonstrated in animal models with commendable success. Along this line, bench-top studies as presented in this article are essential as, to this date, no animal model exists to study chronic single-ventricle physiology and compare efficacy of various cavopulmonary assist alternatives in moderate to long-term postoperative period. Our study confirms that mechanical assist in Fontan circulation incorporating VADs on either the systemic venous bed or at the pulmonary arteries provides cardiopulmonary flow augmentation. After Medos VAD insertion, both RPA and LPA pressure increased approximately 3–9 mm Hg. These results indicate that present pressure head values increases pulmonary arterial flow significantly. In normal physiology, this translates to improved ventricular preload, creating higher cardiac output which, in certain circumstances, aids both immediate and long-term postoperative hemodynamics of functionally normal and "failing" Fontan patients. On the other hand, the flow delay and excessive pressure (10–20 mm Hg) caused by the Pediaflow VAD on its anastomosis branch is associated with the nature of the anastomosis used that were clearly suboptimal for the patient physiology analyzed in this study. Regardless of this design issue, the hemodynamic adjustments in the cavopulmonary circulation still provided a considerable level of pulmonary flow increase with the Pediaflow VAD.

VAD deployment configuration (IVC vs. RPA)

The Medos VAD displayed similar performance in both RPA and IVC segments, although the IVC

TABLE 3. *Variation of the hemodynamic parameters in response to different VAD insertions relative to "Failing Fontan" conditions*

VAD configurations	QIVC (%)	QSVC (%)	QRPA (%)	QLPA (%)	QCV (%)	QPA (%)	ΔPIVC (mm Hg)	ΔPSVC (mm Hg)	ΔPRPA (mm Hg)	ΔPLPA (mm Hg)
SVB										
Medos VAD	66	41	12	19	52	16	0.0	2.1	0.0	0.3
Pediaflow VAD	–25	71	–18	–16	29	–17	6.3	14	4.0	10
PVB										
Medos VAD	57	49	15	10	51	12	5.2	7.5	2.4	6.7
Pediaflow VAD	54	55	–45	100	55	28	8.8	24	9.3	11

Q and ΔP indicate the percent flow variation and absolute pressure head change at the corresponding branch, respectively.

Colour

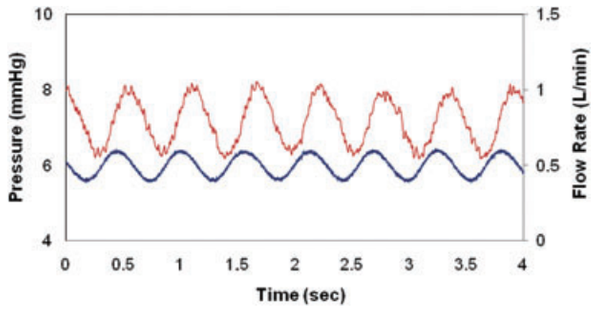

21

FIG. 3. Sinusoidal RPA flow (red) and pressure (blue) waveforms for unassisted circulation under normal physiological conditions.

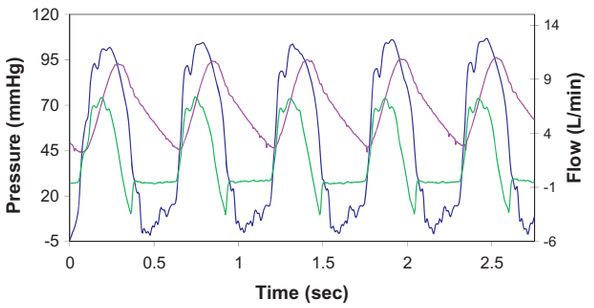

Colour

FIG. 4. Left ventricular pressure (blue), aortic pressure (red), and aortic flow (green) waveforms. Aortic waveforms were similar for both all VAD experiments.

and agrees with previous clinical (21) and computational (22) data.

The significant hemodynamic readjustments and volume shifts that took place with the introduction of assisted support compared with the baseline single-ventricle circulation are summarized in Table 2 qualitatively. Under normal vascular tone, insertion of the Medos pulsatile VAD to IVC in SVB configuration increased the flow within the IVC, SVC, LPA, and RPA segments by 120, 63, 43, and 61%, respectively. Increased IVC flow is accompanied with elevated pressure and larger fluid volume shifted to the IVC compartment. Anastomosis of Medos VAD to the RPA resulted in higher RPA flow (57%) and pressure (95%). In addition, based on the novel "*ejector effect*" of the PAB at RPA, the pressure at the left atrium, venous pressure (IVC and SVC), and also LPA increased considerably (3–8 mm Hg). This caused significant flow augmentation at the LPA segment (37%) and volume shift toward pulmonary artery compartments. Under pulmonary hypertension, flow through the TCPC circuit was increased slightly (3–8%) relative to the normal conditions. Moreover, the blood volume shifted from pulmonary to systemic venous compartments causing venous congestion agrees with clinical observations. Medos VAD insertion to restore pulmonary flow obstruction, not only enhanced the systemic venous flow about 51%, but also increased PA flow about 12–16% compared with the hypertensive levels. To note, both VAD deployment configurations (i.e., IVC and RPA insertion) yielded similar hemodynamic improvements during pulmonary hypertension. The average pressure head added by the Medos VAD on the

TABLE 2. *Configurations investigated the Fontan flow loop*

Configuration	pVAD used	Observations: Hemodynamic	Observations: Volume shifts
1.0) Normal Fontan	None	Baseline	Baseline
1.1) SVB (IVC → TCPC)	1.1.1) Medos VAD	• QIVC ↑, PIVC ↑ • QSVC ↑, PSVC ↑ • QRPA ↑, PRPA ↑ • QLPA ↑, PLPA ↑	• Intermittent volume increase in IVC compartment
	1.1.2) Pediaflow Gen-0 VAD	• QIVC ↓, PIVC ↑ • QSVC ↑, PSVC ↑ • QRPA remained constant, PRPA ↑ • QLPA remained constant, PLPA ↑	• Rapid volume increase in IVC compartment
1.2) PAB (RPA → Left Atrium)	1.2.1) Medos VAD	• QIVC ↑, PIVC ↑ • QSVC ↑, PSVC ↑ • QRPA ↑, PRPA ↑ • QLPA ↑, PLPA ↑	• Intermittent volume increase in RPA compartments
	1.2.2) Pediaflow-Gen-0 VAD	• QIVC ↑, PIVC ↑ • QSVC ↑, PSVC ↑ • QRPA ↓, PRPA ↑ • QLPA ↑, PLPA ↑	• Rapid volume increase in IVC and RPA compartments

Pressure (P) and flow (Q) data were collected with and without two ventricular assist devices (VADs) in two anastomotic configurations; systemic venous booster (SVB) and pulmonary venous booster (PVB); and for two settings of pulmonary compliance ("normal" and "hypertensive").

TABLE 1. *Vascular parameters of the mock system simulating postoperative Fontan circulation in normal and hypertensive conditions*

Parameter	Normal Fontan circulation	Hypertensive circulation
C_{SAB}	0.34	0.34
C_{IVC}	10	10
C_{SVC}	10	10
C_{PAB}	0.78	0.1
C_{PVB}	10	10
$R_{SAB\text{-}L}$	16	12
$R_{SAB\text{-}U}$	12	9
R_{IVC}	10	7.5
R_{SVC}	8	6
R_{PAB}	1.7	1.275
R_{PVB}	0.1	0.075

Shown are the parameters implemented on the mock loop. Parameters are taken from patient data presented in Ref. (12) and Ref. (5).

C, compliance (mL/mm Hg); R, resistance (mm Hg L/min); SAB, systemic arterial bed (-L, lower; -U, upper); SVB, systemic venous bed; PVB, pulmonary venous bed; PAB, pulmonary arterial bed; PVB, pulmonary venous bed.

Life Sciences, Irvine, CA, USA) attached to a six-channel differential amplifier (WPI Inc., Sarasota, FL, USA) in full bridge configuration. In-chamber pressure measurements were validated by conducting simultaneous measurements at locations before, inside, and after the chambers using *in-line* pressure ports. The pressure drop across each chamber is found around 2.5–3 mm Hg. Flow rate through each tubing segment was measured using transonic flow probes (9XL, Transonic Inc., Ithaca, MA, USA). A dedicated data acquisition module NI USB-6229 (NI Inc., Austin, TX, USA) with 16-bit resolution and multiplexing capabilities was employed for sampling and recording data. Distilled water ($\rho = 998$ kg/m^3) was used as the working fluid.

Impedance matching and initial calibration

Combined vascular resistance and compliance constitutes the impedance of a particular vessel segment is given below,

$$Z = R + \frac{1}{i\omega C} \quad (1)$$

where Z, R, C, ω are the complex impedance, resistance, compliance of the vessel segment, and the associated flow waveform, respectively. In order to modulate the vascular impedance in a predictable manner, systemic calibration studies were conducted before the experiments. R and C of each vessel segment are characterized individually to accurately produce the desired normal and abnormal flow conditions. Vascular resistances are adopted from a recent study (12) which incorporated 40 SV patients (age: 6–18), whereas, the compliances assigned to each vessel segment replicated the physiological range available in clinical reports (15,16) and literature (5,17–19) (See Table 1). In order to demonstrate how accurately the vascular resistances can be set using the clamp-type needle pinch valves, we conducted flow and pressure drop measurements at each vessel segment adjusting the pinch valves to different vascular resistances. The resistance data from this calibration were fit to a power regression equation ($Log(R) = 5.3073 + -6.5302$ Log(meter-scale value), $R^2 = 0.889$).

Experimental procedure

Ejection function and cardiac output were set to 45% (20) and 1.6 L/min, respectively to represent the typical post-Fontan hemodynamics. Experiments incorporated a Medos pulsatile VAD (Medos Medizintechnik AG, Stolberg, Germany) with 10 mL stoke volume and a Gen-0 prototype of the Pediaflow centrifugal VAD (PediaFlow Consortium, Pittsburgh, PA, USA) with 350 mL/min flow rate. Alternative to the classical systemic support and total-heart-support configurations, two venous assist scenarios, with single VADs, were explored: the systemic venous booster (SVB) and pulmonary artery booster (PAB) (Fig. 1). Introduced by Rodefeld et al. (9), the SVB refers to VAD anastomosis between the IVC and the TCPC, whereas, in the PAB a VAD is inserted in line between the TCPC and the RPA. Each VAD, anastomosed in both deployment configurations, was analyzed under physiologically normal conditions in order to evaluate the feasibility of mechanical support to improve postoperative Fontan hemodynamics. Experiments are repeated under pulmonary hypertension to evaluate mechanical assist as an aid for "failing" Fontan hemodynamics. In the bench-top loop, pulmonary hypertension is simulated with increased pulmonary resistance and loss of vascular compliance on the LPA and RPA compartments.

RESULTS

Unassisted Fontan circulation experiments produced sinusoidal pulsatile waveforms in both systemic and pulmonary venous compartments for both normal and hypertensive conditions (Fig. 3). Physiological aortic pressure and flow waveforms were produced in all experiments (Fig. 4). The variation of flow in the RPA and IVC segments; and LPA and SVC segments were proportional. This state is associated to the surgical design of the 1DO TCPC model

which comprises a modular pulsatile pump that can run in either SV or biventricular mode selectively. Each ventricular chamber incorporates inflow (mitral/tricuspid) and outflow (aortic/pulmonary) valves. The system further consists of trapped air compliance chambers, variable resistance flow clamps, and the prototype extra-cardiac total cavopulmonary connection anatomy.

For analytical purposes, the mock system elements are designed in six different compartments analogous to the recent electric circuit analog lumped-parameter models developed by our group (5,12) to investigate congenital heart diseases. Pulmonary obstructive disease and hypertension common in "failing" Fontan patients is simulated adjusting the pulmonary artery impedance taken from the clinical data. The mock system includes the left atrium, left ventricle, aorta, inferior and superior vena cava (IVC and SVC), left and right pulmonary arteries (LPA and RPA) to compose systemic circulation and pulmonary circulations (Fig. 2). Ventricular pumping action is simulated using a modified bellows metering pump (GRI Inc., Bellville, OH, USA) with variable stroke volume (20–40 mL) driven by a crank mechanism and shaded pole motor (104 bpm). Low resistance heart valves are constructed in-house from 0.005-m thin shim stock and a polypropylene supporting mesh *sandwiched* between two polyacetal rings and mounted at the inlet and outlet of the bellows chamber. Each compliance chamber was fabricated using closed acrylic tubes with an internal diameter of $3^1/_4$ inches equipped with luer and barbed connectors to connect cannulas or pressure transducers. Hence, this versatile design allows insertion of pediatric assist devices in several anastamotic configurations to analyze multiple postoperative clinical scenarios compared with the same baseline state. The circulation system between the pump and chambers is modeled using transparent Tygon tubing with 3/8″ diameter on the arterial side and 3/4″ diameter on the venous side to match the baseline vascular resistances reported for typical pediatric circulation (Table 1). Clamp-type needle pinch valves (Flow-rite Controls Inc., Byron Center, MI, USA) with a metered scale were installed on each vessel segment to accurately set the resistance in the venous and arterial segments. The change in vascular resistance was determined from regression analyses of time averaged flow and pressure data.

In order to represent the final surgical stage of the Fontan procedure, idealized pyrex glass models of the total cavopulmonary connection (TCPC) was fabricated based on the anatomic MRI data of an 8-year-old TCPC patient (13), where the IVC was anastomosed to the RPA across the SVC with zero and one diameter offset configurations. Both models had idealized planar vessel conduits with a constant inner diameter of 13.4 mm. Flared connections with a radius of curvature of 6.7 mm were employed at the intersection of the vena cavae and the pulmonary arteries to improve the efficiency of TCPC geometry (14). One diameter offset TCPC results are reported in this article.

Pressure measurements were performed at each compliance chamber. Hence, six simultaneous pressure measurements were performed using TruWave disposable pressure transducers (Edwards

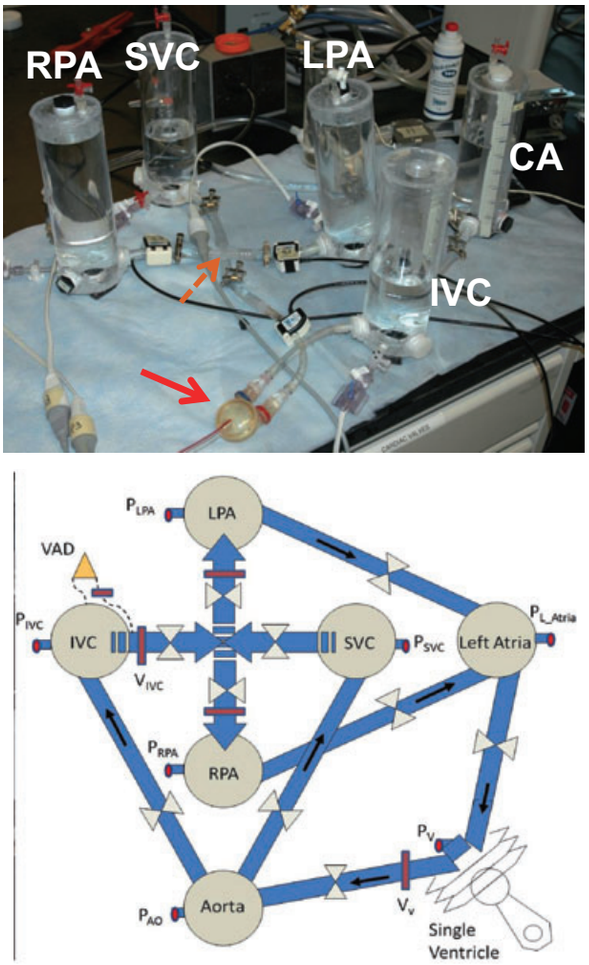

FIG. 2. Schematic representation of the Fontan flow mock loop (bottom) with ventricle assist device attached to IVC and TCPC in series: systemic venous booster (SVB). The compliance chambers are represented by dark grey circles. The grey double-triangles, orange rectangles, and the red circles represent the needle pinch resistors, velocity, and pressure measurement ports, respectively. Medos VAD inserted in SVB configuration and TCPC model are marked by solid red and dashed orange arrows on the flow loop picture (top), respectively.

which comprises a modular pulsatile pump that can run in either SV or biventricular mode selectively. Each ventricular chamber incorporates inflow (mitral/tricuspid) and outflow (aortic/pulmonary) valves. The system further consists of trapped air compliance chambers, variable resistance flow clamps, and the prototype extra-cardiac total cavopulmonary connection anatomy.

For analytical purposes, the mock system elements are designed in six different compartments analogous to the recent electric circuit analog lumped-parameter models developed by our group (5,12) to investigate congenital heart diseases. Pulmonary obstructive disease and hypertension common in "failing" Fontan patients is simulated adjusting the pulmonary artery impedance taken from the clinical data. The mock system includes the left atrium, left ventricle, aorta, inferior and superior vena cava (IVC and SVC), left and right pulmonary arteries (LPA and RPA) to compose systemic circulation and pulmonary circulations (Fig. 2). Ventricular pumping action is simulated using a modified bellows metering pump (GRI Inc., Bellville, OH, USA) with variable stroke volume (20–40 mL) driven by a crank mechanism and shaded pole motor (104 bpm). Low resistance heart valves are constructed in-house from 0.005-m thin shim stock and a polypropylene supporting mesh *sandwiched* between two polyacetal rings and mounted at the inlet and outlet of the bellows chamber. Each compliance chamber was fabricated using closed acrylic tubes with an internal diameter of $3^1/_4$ inches equipped with luer and barbed connectors to connect cannulas or pressure transducers. Hence, this versatile design allows insertion of pediatric assist devices in several anastamotic configurations to analyze multiple postoperative clinical scenarios compared with the same baseline state. The circulation system between the pump and chambers is modeled using transparent Tygon tubing with 3/8″ diameter on the arterial side and 3/4″ diameter on the venous side to match the baseline vascular resistances reported for typical pediatric circulation (Table 1). Clamp-type needle pinch valves (Flow-rite Controls Inc., Byron Center, MI, USA) with a metered scale were installed on each vessel segment to accurately set the resistance in the venous and arterial segments. The change in vascular resistance was determined from regression analyses of time averaged flow and pressure data.

In order to represent the final surgical stage of the Fontan procedure, idealized pyrex glass models of the total cavopulmonary connection (TCPC) was fabricated based on the anatomic MRI data of an 8-year-old TCPC patient (13), where the IVC was anastomosed to the RPA across the SVC with zero and one diameter offset configurations. Both models had idealized planar vessel conduits with a constant inner diameter of 13.4 mm. Flared connections with a radius of curvature of 6.7 mm were employed at the intersection of the vena cavae and the pulmonary arteries to improve the efficiency of TCPC geometry (14). One diameter offset TCPC results are reported in this article.

Pressure measurements were performed at each compliance chamber. Hence, six simultaneous pressure measurements were performed using TruWave disposable pressure transducers (Edwards

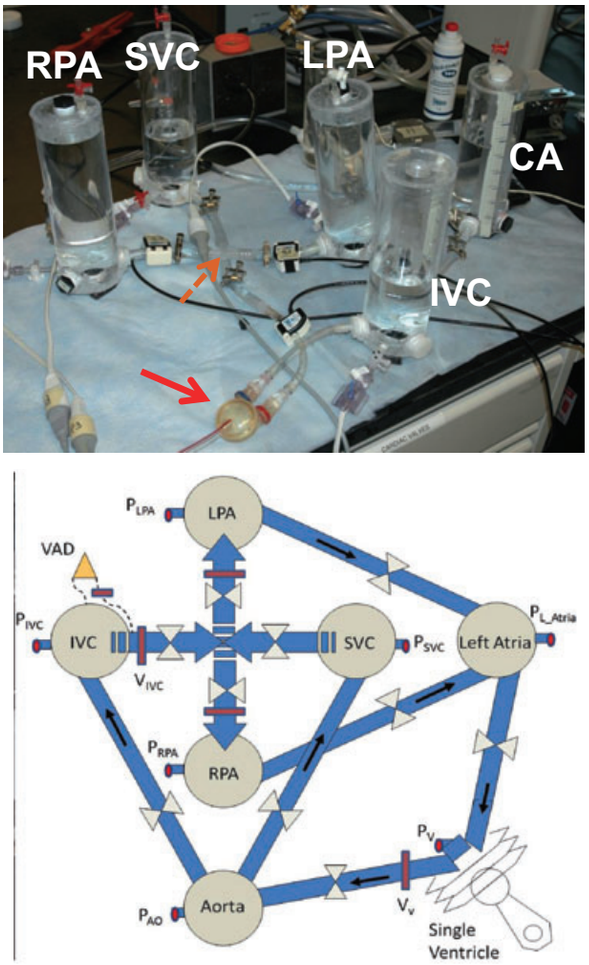

FIG. 2. Schematic representation of the Fontan flow mock loop (bottom) with ventricle assist device attached to IVC and TCPC in series: systemic venous booster (SVB). The compliance chambers are represented by dark grey circles. The grey double-triangles, orange rectangles, and the red circles represent the needle pinch resistors, velocity, and pressure measurement ports, respectively. Medos VAD inserted in SVB configuration and TCPC model are marked by solid red and dashed orange arrows on the flow loop picture (top), respectively.

ventricular preload, and reverse the Fontan Paradox of underfilling of the pulmonary arteries with hypertension in the pulmonary capillaries. Several opportunities exist for a VAD system to improve patient outcomes during both immediate postoperative and late "failing" states of the disease. Preliminary data in humans and animals support the feasibility of circulatory assist (8,9), however, a major deficit is that the current studies implement the conventional VAD systems that are not specially designed for utilization as booster pumps in lower-pressure flow assist scenarios. The idea of Fontan VAD contrasts sharply with the traditional concept of a left or right ventricular assist device (LVAD or RVAD) that generally takes over the circulatory responsibilities from a damaged ventricle.

Many VAD programs have investigated standard flow loops focusing only on the systemic compartments for testing device performance both in continuous (10) and pulsatile (10,11) modes. Although these simple systems allow for the assessment of VAD performance for conventional physiologies, few are able to mimic the hemodynamic conditions of nontraditional physiologies, such as the Fontan patients, and thus provide limited insight on the effectiveness of VAD insertion for patients with congenital heart defects. In vitro set-ups for Fontan patients are scarce and have been limited to steady venous flow conditions that emphasize the use of devices as a left ventricular support and generally ignore the effects of the surgically constructed pulmonary conduit on venous return, fluid balance, and cardiac function in the SV. A reliable bench-top pediatric single-ventricle pulsatile flow loop is necessary to investigate the feasibility of using VADs other than as a LVAD in the postoperative period. Using the VAD in a fashion that simultaneously reduces venous stasis and restores cardiac output may reduce postoperative morbidity and prove to be superior to the current LVAD paradigm which most directly addresses the problems associated with ventricular overloading associated with poor ventricular performance. The ideal experimental workbench should enable systemic evaluation and optimization of assisted circulation strategies for short or moderate term VAD use in "failing" Fontans as well. The goal of mechanical support for Fontan patients should translate from decreasing the workload of the SV to extending the life of the entire cardiopulmonary circuit and thereby extending the time that patients may be bridged to transplant on VAD support.

The pediatric mock circulation system introduced in this study reproduced physiological and pathological states (pulmonary hypertension) with realistic hemodynamics. Our results demonstrated its utility to simulate the Fontan circulation and the hemodynamic effects of insertion of various existing VADs. The present bench-top flow loop was designed with the objective of (i) reproducing both the physiological and pathological conditions that are commonly observed during the early and long-term postoperative life after Fontan procedure; and (ii) evaluation of the feasibility of cardiopulmonary support in single-ventricle patients. Likewise, the proposed flow loop should facilitate the deployment of alternative PVAD anastomosis configurations (Fig. 1). Particularly the present flow loop design (i) allows tuning of the vascular resistance and compliance of the individual arterial and venous compartments within the clinical ranges; (ii) provides an ability to adjust patient-specific pediatric flow rate; and (iii) allows practical insertion of PVADs, data acquisition instruments (pressure-flow probes), and anatomical Fontan models.

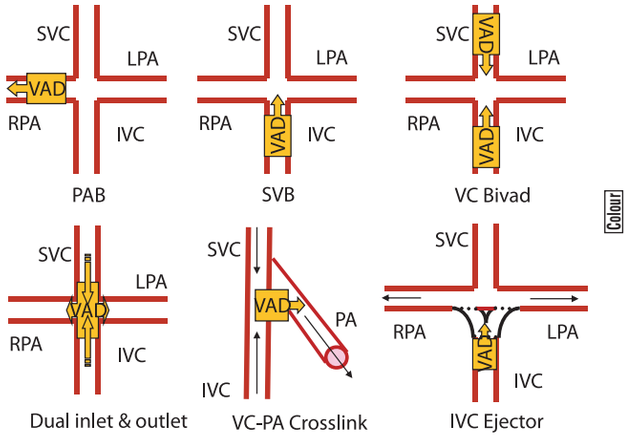

FIG. 1. A cartoon of possible venous ventricle assist device configurations (VAD) for cardiopulmonary support in Fontan patients. VADs are inserted (from top left to bottom right) between pulmonary artery-to-venous bed (pulmonary artery booster-PAB), systemic venous return-to-TCPC (systemic venous booster-SVB), dual caval veins-TCPC (CV-Bivad) (9), double-inlet double outlet (5), vena cava to pulmonary arteries crosslink (uses a VAD with a single inlet and outlet to connect between the two vessels), IVC ejector pump. In this study, SVB and PAB configurations are studied. SVC, IVC, RPA, LPA refer to superior vena cava, inferior vena cava, right and left pulmonary artery, respectively.

MATERIALS AND METHODS

Mock circulation loop

The entire SV Fontan circulation is modeled in vitro by constructing a bench-top pediatric flow setup